Optical properties under exposure to ultrashort laser pulses

2002 J. Phys.: Condens. Matter 14 6689

(http://iopscience.iop.org/0953-8984/14/26/309)

INSTITUTE OF PHYSICS PUBLISHING JOURNAL OF PHYSICS: CONDENSED MATTER

J. Phys.: Condens. Matter **14** (2002) 6689–6700 PII: S0953-8984(02)35821-1

Optical properties under exposure to ultrashort laser pulses

Bernd Hüttner

Institute of Technical Physics, DLR, Pfaffenwaldring 38–40, 70569 Stuttgart, Germany

Received 21 April 2002, in final form 13 May 2002
Published 21 June 2002
Online at stacks.iop.org/JPhysCM/14/6689

Abstract

For the description of the interaction of a femtosecond laser pulse with a solid, the standard values of the properties of a solid are not suited because they have been experimentally determined or theoretically derived under the assumptions of a steady state and local thermal equilibrium. Depending on the property considered and the laser pulse duration, either one or both of these conditions may be violated. This is caused by the appearance of a local thermal nonequilibrium, a nonsteady state, and the possibly large difference between the temperatures of the electron and phonon subsystems.

For a deeper understanding and for the prediction of experimental results, it is essential to have knowledge of the optical properties, and especially of the absorption and of the optical penetration depth, on the fs timescale. In this paper, we derive equations for the optical properties of metals in the case of local thermal nonequilibrium between the electron and phonon systems. For given laser intensities, we calculate, as an example, the optical properties for gold. For this purpose, we need the time-dependent temperatures of the electrons and phonons. They are evaluated by means of our extended two-temperature model. Finally, we compare the results with the standard equilibrium behaviour as well as with the experimental findings and close with a short discussion.

1. Introduction

Knowledge of the absorption and the optical penetration depth during the interaction of a laser pulse with metals is important both for modelling and applications. In the case of long laser pulses, one can simply take the needed information from compilations where, for example, the reflectivity and the absorption coefficient are listed as functions of frequency and temperature. For ultrashort laser pulses, however, these values become doubtful because they are usually determined under the conditions of local thermal equilibrium and a steady state. Since these assumptions are violated for pulses in the fs and partly also in the ps range, we have to expect deviations from the standard behaviour. This statement is supported both by experiments on transient thermal reflectivity (Sun *et al* 1994, Bonn *et al* 2000) and also by investigations of

0953-8984/02/266689+12$30.00

the change in the behaviour of the thermal properties (Hüttner 1998). Indeed, the electrons may have a temperature which is not only much higher than that of the phonons, but also even higher than any value under which a solid or liquid state could exist.

In addition, as traditional solid-state physics is also based on the two above-mentioned conditions, one has to use a nonequilibrium approach for the calculation of the optical properties.

The first task, the determination of the electron distribution function $f(\vec{k}, t)$, for local thermal nonequilibrium was solved in Hüttner (1999). There, we derived $f(\vec{k}, t)$ by a perturbation treatment of the Boltzmann equation together with an additional photon operator. In the following, we will use this function for the calculation of the frequency-dependent electrical conductivity.

2. Electrical conductivity

For an electron gas interacting with laser radiation, the Boltzmann equation may be written as

$$\frac{\partial f(\vec{k},t)}{\partial t} + \vec{v}\frac{\partial f(\vec{k},t)}{\partial \vec{r}} - e\vec{v}\cdot\vec{E}\frac{\partial f(\vec{k},t)}{\partial E} = \int P(\vec{k},\vec{k}',t)[f(\vec{k}',t) - f(\vec{k},t)]\,\mathrm{d}\vec{k}' - \nu G(f(\vec{k},t)) \tag{1}$$

where all terms, except for the last one, have their usual meaning. The additional term represents the phonon-assisted absorption or emission of photons. It depends essentially on the absorbed intensity including its time dependence, the electron density, the absorption coefficient, and the laser frequency. A detailed discussion can be found in Hüttner (1999). Briefly, equation (1) is solved by expanding f in a power series in the small parameter $p = \nu\tau$, defined by

$$p(t) = \nu(t)\tau = \frac{I(t)\tau}{n\hbar\omega\delta}. \tag{2}$$

Here, for the reader's convenience, we give only the first- and (further below) second-order solutions to equation (1). Assuming that the electron temperature is well established, which implies a lower boundary for the laser pulse duration τ_L of about 100 fs, we find in first order

$$pf_1 = \mathrm{e}^{-t/\tau}\int_{-\infty}^{t}\mathrm{d}t'\,\mathrm{e}^{t'/\tau}\left[\left\{e\vec{v}\cdot\vec{E}_0\mathrm{e}^{-\mathrm{i}\omega t}h(t)\left(\frac{\partial f_0}{\partial E}\right) - (\vec{v}\cdot\vec{\nabla}T - \dot{T})\left(\frac{\partial f_0}{\partial T}\right)\right\} + \nu_0 H(t)G(f_0)\right] \tag{3}$$

with f_0 as the Fermi–Dirac distribution function and $H(t)$ as the time envelope function of the laser pulse. The abbreviation ν_0 follows from equation (16) when $I(t)$ is replaced by I_0. The function $h(t)$ of the electric field is defined by $I(t) \sim |E(t)|^2 \sim H(t)|E|^2 \sim |h(t)E|^2$.

Evaluating the integral, we get

$$pf_1 = -\left\{\frac{e\tau\vec{v}\cdot\vec{E}_0}{1-\mathrm{i}\omega\tau}\mathrm{e}^{-\mathrm{i}\omega t}h(t) + (E-\mu)\vec{v}\tau\cdot\frac{\vec{\nabla}T}{T}\right\}\left(-\frac{\partial f_0}{\partial E}\right) + p_0 H(t)G(f_0) \tag{4}$$

with the expansion parameter $p_0 = \nu_0\tau$ corresponding to the number of absorbed photons during the scattering time τ, and μ being the temperature-dependent chemical potential. The scattering rate $\tau(E, T_e, T_{ph})^{-1}$ is composed of the sum of the rates for electron–phonon and electron–electron scattering. Within the framework of the Fermi liquid theory, we can write it as

$$\tau^{-1} = \tau_{ph}^{-1} + \tau_{e-e}^{-1} = \tau_{ph}^{-1} + \tau_T^{-1} + \tau_E^{-1} = \tau_{ph}^{-1} + 4\pi^2\beta T_e^2 + \beta(E-\mu)^2 \tag{5}$$

where β is an experimental parameter (Parkins *et al* 1981).

2.1. First-order contribution

In first order, the electrical current density is defined by

$$\vec{j}_{e1} = \sigma_1 \vec{E} = -e \sum \vec{v} p f_1. \tag{6}$$

Taking into account that odd powers of the velocity vanish, and using the condition $\tau \ll \tau_L$, we obtain from equations (4) and (6) for the current density

$$\vec{j}_{e1} = \vec{j}_{\vec{E}1} + \vec{j}_{T1} = e \sum_{\vec{k}} \frac{\vec{v}^2 e\tau}{(1 - \mathrm{i}\omega\tau)} \vec{E}_0 \mathrm{e}^{-\mathrm{i}\omega t} h(t) \left(-\frac{\partial f_0}{\partial E} \right) + e \sum_{\vec{k}} (E - \mu) \vec{v}^2 \tau \frac{\vec{\nabla} T}{T} \left(-\frac{\partial f_0}{\partial E} \right). \tag{7}$$

Both contributions to the current density are linearly independent if the incidence of the laser radiation is parallel to the surface normal, because the electric field is perpendicular to the thermal gradient in this case. Furthermore, since the time dependence of the electron temperature is related to the laser pulse duration, we can consider j_T as a constant in comparison with the fast time dependence of j_E. For this reason, the thermal part does not give a direct contribution to $\sigma(\omega)$. Therefore, we neglect it in the following.

Depending on the electron temperature, three cases may be considered for the frequency-dependent conductivity.

Case 1. $T_e = T_{ph}$, $\tau_{ph} = \tau_D \ll \tau_{e-e}$ (where τ_D is Drude's scattering time). Here,

$$\begin{aligned}
\sigma(\omega, T_{ph}) &= e^2 \sum_{\vec{k}} \frac{\vec{v}^2 \tau_D}{(1 - \mathrm{i}\omega\tau_D)} \left(-\frac{\partial f_0}{\partial E} \right) h(t) \\
&= \frac{e^2 \tau_D}{(1 - \mathrm{i}\omega\tau_D)} h(t) \int \frac{\mathrm{d}\vec{k}}{4\pi^3} v^2 \left(-\frac{\partial f_0}{\partial E} \right) \\
&= \frac{e^2 \tau_D}{(1 - \mathrm{i}\omega\tau_D)} \frac{3n}{2\mu_0^{3/2}} \int \mathrm{d}E \sqrt{E} v^2 \left(-\frac{\partial f_0}{\partial E} \right) h(t) \\
&= \frac{e^2 \tau_D n}{m} \frac{h(t)}{(1 - \mathrm{i}\omega\tau_D)} = \sigma_D \frac{h(t)}{(1 - \mathrm{i}\omega\tau_D)}.
\end{aligned} \tag{8}$$

The function $h(t)$ appears in equation (8) because this term can be extracted from the time integral in equation (3). Justification for this approximation is provided by the features that

(i) the function $h(t)$ is slowly varying in comparison with the fast exponential term and
(ii) numerical calculations of the difference between the complete and the approximated expressions deviate by $<1\%$.

Case 2. $\tau_D < \tau_{e-e}$, $T_e > T_{ph}$. For convenience, we rewrite equation (5) in the form

$$\tau(E, T_e, T_{ph}) = \frac{\tau_{ph}(T_{ph})}{1 + z(T_e, T_{ph}) + \tau_{ph}(T_{ph}) \beta (E - \mu(T_e))^2} \tag{9}$$

where the function $z(T_e, T_{ph})$ is defined by the ratio of the electron–phonon scattering time over part of the electron–electron scattering time, depending on the temperature:

$$z(T_e, T_{ph}) = \frac{\tau_{ph}(T_{ph})}{\tau_T(T_e)} = 4\pi^2 \beta T_e^2 (eV) \tau_{ph}(T_{ph}). \tag{10}$$

For the conductivity, we get now

$$\sigma = \frac{e^2}{2\mu^{3/2}} \frac{3n}{} \int \mathrm{d}E \sqrt{E} v^2 \frac{\tau_D}{1 + z + \tau_D \beta [E - \mu]^2 - \mathrm{i}\omega\tau_D} \left(-\frac{\partial f_0}{\partial E} \right). \tag{11}$$

For $k_B T_e \ll \mu_0$, we can make the approximation $(-\partial f_0/\partial E) \cong \delta(E-\mu_0)$ and finally find

$$\sigma(\omega, T_e, T_{ph}) = \sigma_D \frac{h(t)}{1+z(T_e, T_{ph}) - \mathrm{i}\omega\tau_D}. \tag{12}$$

Equation (11) improves Drude's theory by taking into account the effect of electron–electron scattering. The magnitude of the effect depends on the value of the parameter β and, of course, on the electron temperature.

Case 3. $\tau_D > \tau_{e-e}$, $T_{ph} \ll T_e$. In this case, we use Sommerfeld's expansion for developing $\mu(T_e)$, and get with the free-electron density of levels from equation (11)

$$\sigma_1(\omega, T_e, T_{ph}) = \frac{\sigma_D}{1+z-\mathrm{i}\omega\tau_D} + \frac{e^2 3n\tau_D}{m\sqrt{\mu}} \frac{\pi^2 T_e^2}{6} \frac{\partial^2}{\partial E^2} \left[\frac{\sqrt{E}}{1+z+\tau_D\beta(E-\mu)^2 - \mathrm{i}\omega\tau_D} \right]\Bigg|_{E=\mu} \tag{13}$$

and finally, after evaluation of equation (13) together with the time function of the electric field,

$$\sigma_1(\omega, T_e, T_{ph}, t) = \sigma_D \Gamma h(t) \left\{ (1+z) \left[1 + \frac{z}{12(1+z)} - \frac{\pi^2 k_B^2 T_e^2}{24\mu_0^2} - \frac{z(1+z)\Gamma}{6} \right] + \mathrm{i}\omega\tau_D \left[1 - \frac{\pi^2 k_B^2 T_e^2}{24\mu_0^2} - \frac{z(1+z)\Gamma}{6} \right] \right\} \tag{14}$$

with σ_D being Drude's dc conductivity and using the new abbreviation

$$\Gamma = \Gamma(\omega, T_e, T_{ph}) = \frac{1}{(1+z(T_e, T_{ph}))^2 + \omega^2\tau_D^2}. \tag{15}$$

Drude's ac conductivity follows from equation (14) in the limits $k_B T_e \ll \mu_0$, $z \to 0$, and $h(t) =$ constant.

2.2. Second-order contribution

The next order is obtained by insertion of equation (4) into the following expression:

$$p^2 f_2 = \mathrm{e}^{-t/\tau} \int_{-\infty}^{t} \mathrm{d}t' \, \mathrm{e}^{t'/\tau} \left\{ -\vec{v}\cdot\vec{\nabla}T \left(\frac{\partial(pf_1)}{\partial T} \right) + e\vec{v}\cdot\vec{E} \left(\frac{\partial(pf_1)}{\partial E} \right) + \nu_0 G H(t)(pf_1) \right\}. \tag{16}$$

Due to the energy and temperature dependence of the relaxation time τ, the solution of the integral becomes rather long. For this reason, we will not give the complete expression here but restrict ourselves to the terms needed for the calculation of the electrical current density. One can considerably reduce the number of integrals by taking into account that the electric current density is proportional to $\Sigma v f$. Therefore, terms containing odd powers of v vanish upon integration over k-space. Furthermore, in agreement with the first-order treatment, we can neglect the terms proportional to ∇T. The remaining integral reads

$$p^2 f_2 \vec{v} = \mathrm{e}^{-t/\tau} \int_{-\infty}^{t} \mathrm{d}t' \, \mathrm{e}^{t'/\tau} \times \left\{ e\vec{v}^2 \vec{E} \mathrm{e}^{-\mathrm{i}\omega t'} \frac{\partial}{\partial E}[p(t)G(f_0)] - \nu_0 \vec{v} G \left[\left\{ \frac{e\tau\vec{v}\cdot\vec{E}\mathrm{e}^{-\mathrm{i}\omega t'}}{1-\mathrm{i}\omega\tau} \right\} \left(-\frac{\partial f_0}{\partial E} \right) \right] \right\}. \tag{17}$$

Solving the integral, we obtain for the electrical current density in second order

$$\vec{j}_2 = e^2 \sum_{\vec{k}} \frac{1}{4\pi^3} \vec{v}^2 \left[\frac{\tau^2\nu_0}{(1-\mathrm{i}\omega\tau)} + \frac{\tau^2\nu_0 h(t)}{(1-\mathrm{i}\omega\tau)^2} \right] G\left(-\frac{\partial f_0}{\partial E} \right) \vec{E}_0 h(t) \mathrm{e}^{-\mathrm{i}\omega t}. \tag{18}$$

From this we get for the real and imaginary parts of the complex conductivity in the free-electron approach

$$\sigma_2' = \sigma_D h(t)\Gamma(\omega, T_e, T_{ph})\, p_0 \left\{ 1 - \frac{\pi^2 T_e^2}{24\mu_0^2} + \frac{1}{6} z(1+z)(h(t)-1) + \Gamma(\omega, T_e, T_{ph})[(1+z)^2 - \omega^2\tau_D^2]\left[1 - \frac{\pi^2 T_e^2}{24\mu_0^2} - \Gamma(\omega, T_e, T_{ph})\frac{z}{3}(1+z) \right] \right\} \tag{19}$$

and

$$\sigma_2'' = \sigma_D \omega \tau_D h(t)\Gamma(\omega, T_e, T_{ph})\, p_0 \left\{ \frac{1}{1+z}\left(1 - \frac{z}{12(1+z)} - \frac{\pi^2 T_e^2}{24\mu_0^2} \right) + \tfrac{1}{6} z(z+1)(h(t)-1)\Gamma(\omega, T_e, T_{ph}) + 2(1+z)\Gamma(\omega, T_e, T_{ph})\left(1 - \frac{\pi^2 T_e^2}{24\mu_0^2} - \frac{z}{3}(1+z)\Gamma(\omega, T_e, T_{ph}) \right) \right\} \tag{20}$$

where p_0 is redefined by $p_0 = \nu_0\, \tau_D = (I_0 \tau_D)/(n\hbar\omega\delta)$ (I_0: peak intensity; n: electron density; δ: absorption depth). The chemical potential is replaced in the expressions by μ_0 because the first correction is proportional to $(k_B T_e/\mu_0)^4$.

Using the familiar relation between the complex dielectric function and the complex ac conductivity,

$$\varepsilon(\omega, T_e, T_{ph}) = \varepsilon_0 + \mathrm{i}\frac{4\pi}{\omega}[\sigma_1(\omega, T_e, T_{ph}) + \sigma_2(\omega, T_e, T_{ph})], \tag{21}$$

we are now able to determine the optical properties for the case of local thermal nonequilibrium up to second order.

Aiming to show the changes for all optical properties, we first make a numerical evaluation, because no paper reporting a closed measurement of the properties is known.

It is worth noting that such a numerical evaluation cannot directly be compared with published transient thermal reflection measurements. This is due to the fact that the theoretical optical properties depend explicitly on the time function of the laser pulse and therefore, for example, the absorption is zero after the pulse. The experiment, however, probes the time dependence of the absorption caused by a preceding pump pulse.

For this purpose, we calculate for gold the time dependences of the surface temperatures of the electron and phonon subsystems with the extended two-temperature model (Hüttner and Rohr 1996) improved by using the nonlinear electronic thermal conductivity derived by Hüttner (1998). The main effect of the nonlinear electron-temperature dependence, which is caused by the electron–electron scattering, is an enhancement of the surface temperatures because the thermal diffusivity is reduced.

For the sake of simplicity, a top-hat profile is used for the time dependence of the laser pulses.

In this way, the intrinsic time dependence of the properties can be assessed more easily, because it is not masked by the shape of the laser pulse. The laser data used for $\omega = 1$ eV and $\tau_L = 500$ fs are $I_{abs} = 10$ GW cm^{-2} and $I_{abs} = 20$ GW cm^{-2}, respectively. The surface temperatures are plotted in figures 1 and 2.

The cusps of the electron temperatures reflect the sharp cut-off of the top-hat profile. In the next step, we use the calculated values of the temperatures as input data for the determination of the electrical conductivity. The resulting curves for the real and imaginary parts are given in figures 3 and 4

At $t = 0$, the difference in behaviour of the two parts of the conductivity is due to the appearance of $(1+z(T_e, T_{ph}))$ in the denominator of the imaginary part, equation (20). Although

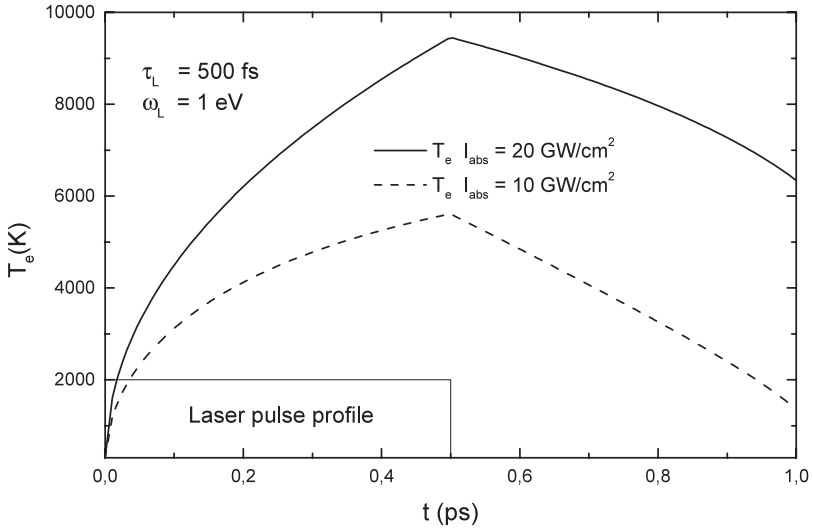

Figure 1. Surface temperatures of the electrons of gold for a top-hat profile with $\omega = 1$ eV, $\tau_L = 500$ fs, and $I_{abs} = 10$ and 20 GW cm^{-2}.

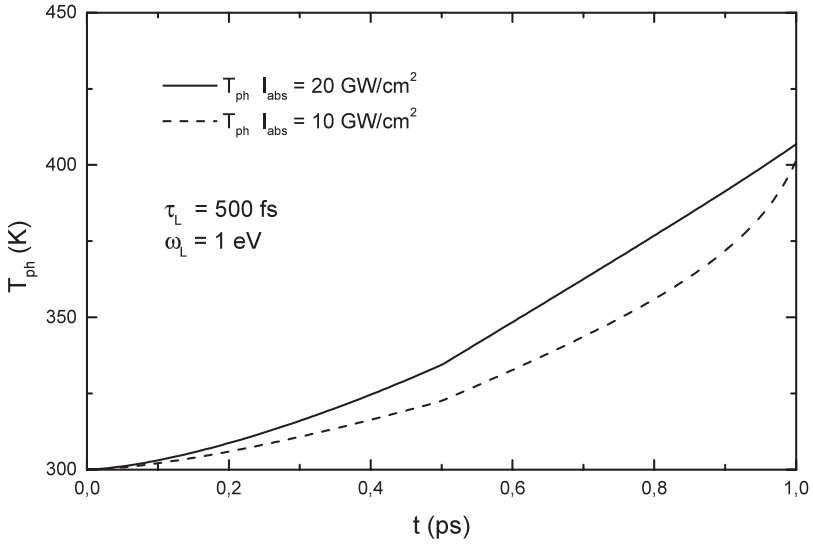

Figure 2. Surface temperatures of the phonons of gold for a top-hat profile.

the electron–electron interaction is small at room temperature, it is already responsible for a deviation from Drude's theory. Furthermore, the strong dependence on intensity is worth noting. While the real part is enhanced by more than one order of magnitude, the decrease of the imaginary part is only about 20%.

A similar behaviour can be seen in the next four figures for the real and imaginary parts of the dielectric function and the refractive index, respectively. As is well known, the real and imaginary parts of the refractive index, respectively, are related to the complex dielectric function by

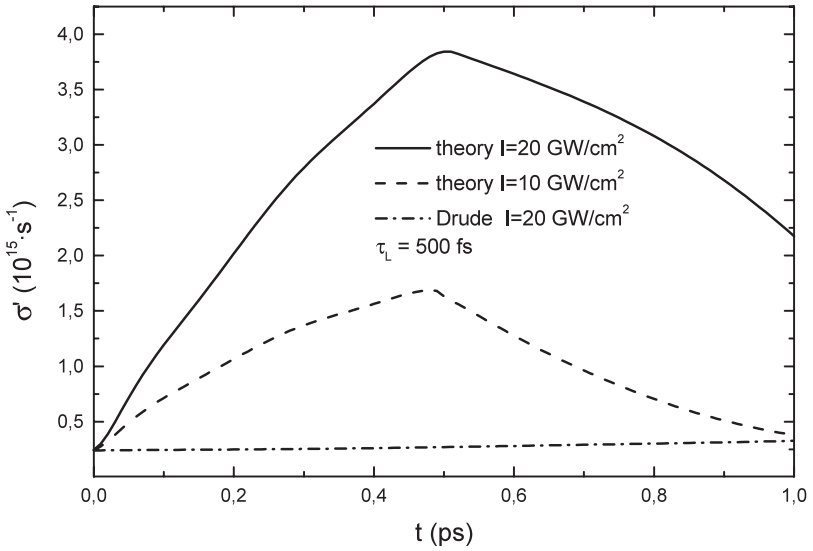

Figure 3. The real part of the electrical conductivity: full and dashed curves display the theory up to second order; the dashed–dotted curve shows Drude's theory.

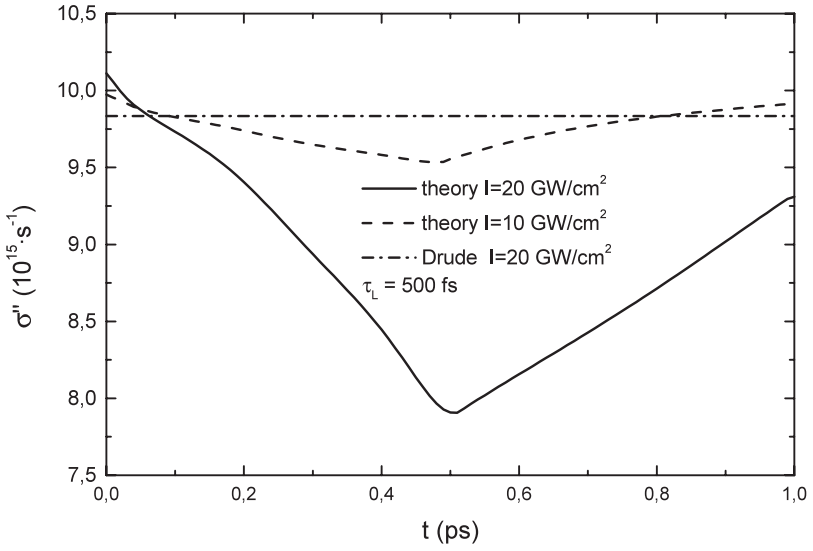

Figure 4. The imaginary part of the electrical conductivity: full and dashed curves display the theory up to second order; the dashed–dotted curve shows Drude's theory.

$$n(\omega, T_e, T_{ph}) = \mathrm{Re}\{\sqrt{\varepsilon(\omega, T_e, T_{ph})}\}, \qquad k(\omega, T_e, T_{ph}) = \mathrm{Im}\{\sqrt{\varepsilon(\omega, T_e, T_{ph})}\}.$$

For convenience and later use, we also give here the expressions for the absorption depth and for the absorption: respectively,

$$\delta(\omega, T_e, T_{ph}) = \frac{c}{\omega k(\omega, T_e, T_{ph})}, \qquad A(\omega, T_e, T_{ph}) = 1 - \left|\frac{\sqrt{\varepsilon(\omega, T_e, T_{ph})} - 1}{\sqrt{\varepsilon(\omega, T_e, T_{ph})} + 1}\right|^2.$$

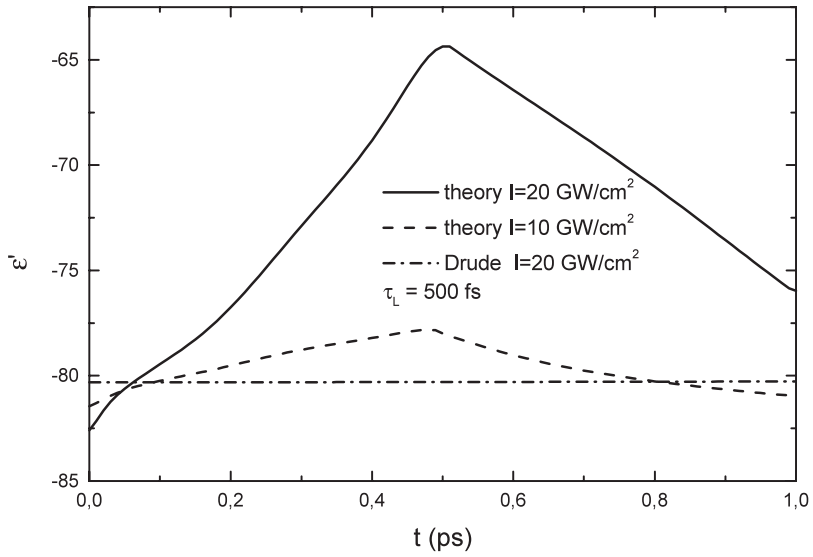

Figure 5. The real part of the dielectric function: full and dashed curves display the theory up to second order; the dashed–dotted curve shows Drude's theory.

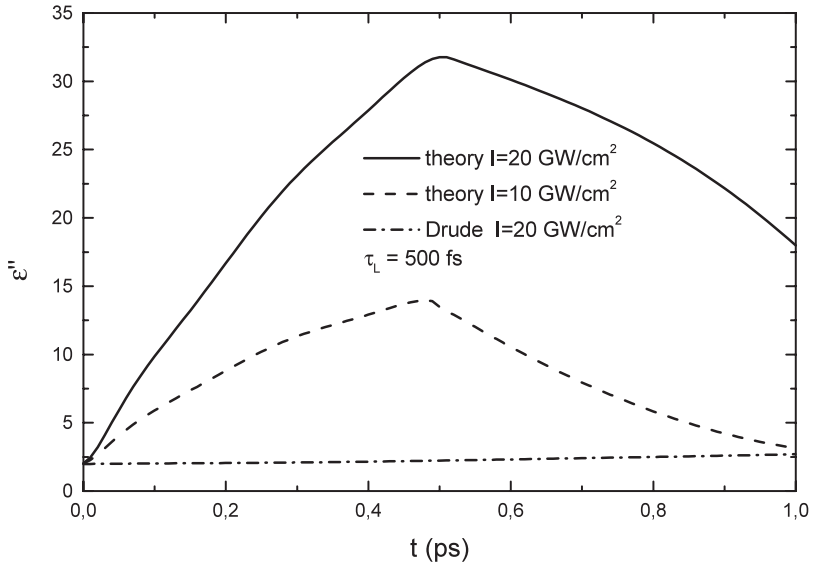

Figure 6. The imaginary part of the dielectric function: full and dashed curves display the theory up to second order; the dashed–dotted curve shows Drude's theory

The most important quantities for applications and simulations, the optical penetration depth and the absorption, are plotted in figures 9 and 10. Both quantities are crucial for the stored laser energy, the resulting energy density in the solid, and, if the latter is large enough, the character of the ablation process.

At first glance, the absorption depth is only slightly changed, about 1% at 10 GW cm^{-2} but already about 10% at 20 GW cm^{-2}. In fact, this strong nonlinear behaviour may result in a dramatic modification at higher intensities.

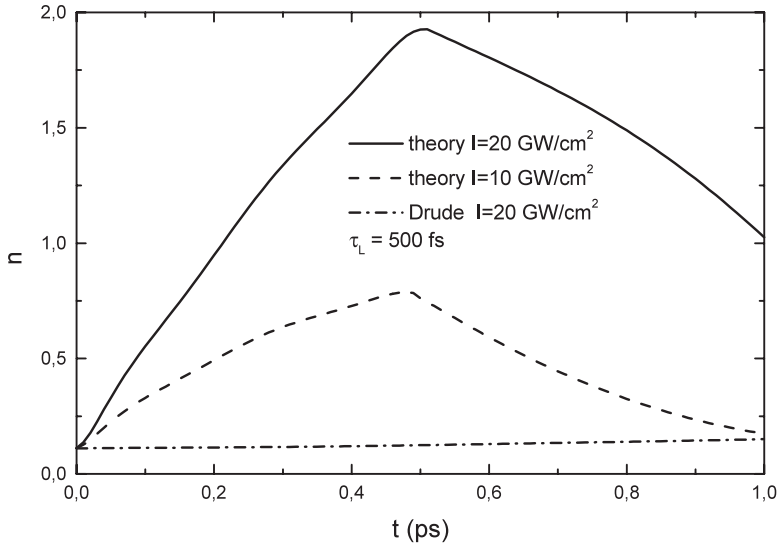

Figure 7. The real part of the refractive index: full and dashed curves display the theory up to second order; the dash–dotted curve shows Drude's theory.

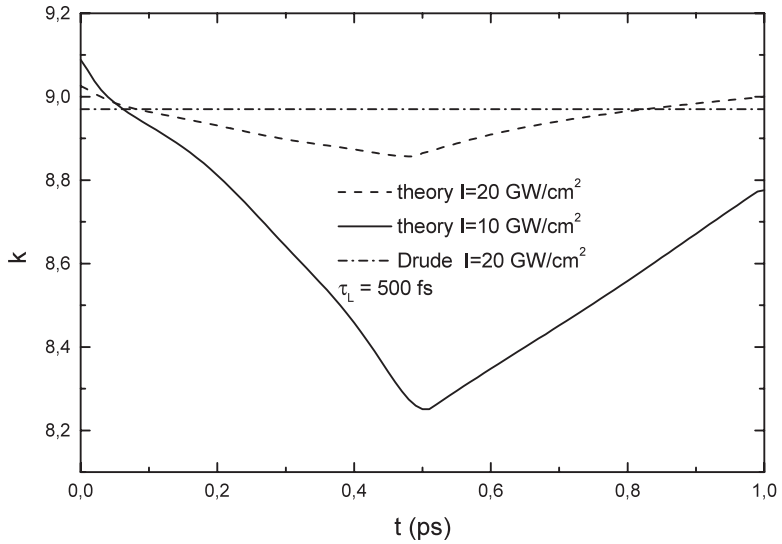

Figure 8. The imaginary part of the refractive index: full and dashed curves display the theory up to second order; the dash–dotted curve shows Drude's theory.

Inspecting figures 3–10, one can recognize the important consequences of the existence of local thermal nonequilibrium for the optical properties of the metal. While in the standard theory the increase of the phonon temperature, more exactly $T = T_e = T_{ph}$, only leads to slight modifications (dash–dotted curves), the properties under fs laser pulses are overwhelmingly dominated by the appearance of a local thermal nonequilibrium between the electrons and phonons (full and dashed curves). At first sight, the similarity of the shapes of the curves suggests that this is mainly caused by how the electron temperature evolves. A closer investigation, however, shows that this is more or less the case for the properties dominated

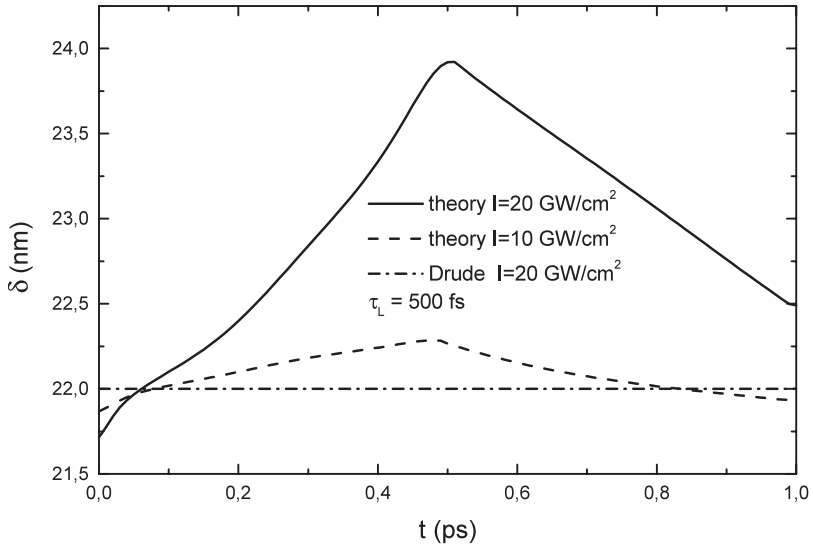

Figure 9. The optical penetration depth in nm: full and dashed curves display the theory up to second order; the dash–dotted curve shows Drude's theory.

Table 1. Relative change, $\Delta x/x = [x(\tau) - x(0)]/x(0)$, of the electron and phonon temperatures (T_e, T_{ph}), the real and imaginary parts of the conductivity (σ', σ''), the dielectric functions (ε', ε'') and the refractive indices (n, k), the absorption depth (δ) and the absorption (A) for $I = 10$ GW cm^{-2} (second line) and $I = 20$ GW cm^{-2} (third line).

$\frac{\Delta T_e}{T_e}$	$\frac{\Delta T_{ph}}{T_{ph}}$	$\frac{\Delta\sigma'}{\sigma'}$	$\frac{\Delta\varepsilon''}{\varepsilon''}$	$\frac{\Delta n}{n}$	$\frac{\Delta A}{A}$	$\frac{\Delta\sigma''}{\sigma''}$	$\frac{\Delta\varepsilon'}{\varepsilon'}$	$\frac{\Delta k}{k}$	$\frac{\Delta\delta}{\delta}$
15.94	0.100	5.67	5.67	5.79	5.88	−0.042	0.042	−0.018	0.018
29.23	0.127	14.73	14.73	16.20	17.59	−0.208	0.210	−0.086	0.094

by the real part of the conductivity. Those properties, which are more directly governed by the imaginary part of the conductivity, show a delicate balance of the contributions from the changes in the electron and phonon temperatures mainly caused by the product $\omega\tau_D(T_{ph})$. The absorption coefficient provides a prime example. Although the change of the imaginary part of the dielectric function is much larger than the change of the real part, as given in table 1, it is not able to compensate for the 'loss' of the real part with increasing phonon temperature. For this reason, the absorption coefficient decreases. This is in complete analogy to the behaviour in the standard theory if the frequency is increased.

Surely the most serious change, an increase by almost a factor of 20, appears in the absorption. Such an enhancement and the corresponding decrease of the reflection have been observed in many experiments (Banyai *et al* 1990, Bonn *et al* 2000, Fedosejevs *et al* 1990, Sun *et al* 1994).

Another important fact is given by the different nonlinear responses of the various optical properties to the changes of the temperatures. A slight increase of the relative change of the phonon temperature by 27% leads to a variation of the relative change of the absorption depth by more than a factor of 5.

Since gold has one of the smallest coefficients of energy exchange, one can expect that this effect may still be larger for other metals provided that the phonon temperature stays below the evaporation point.

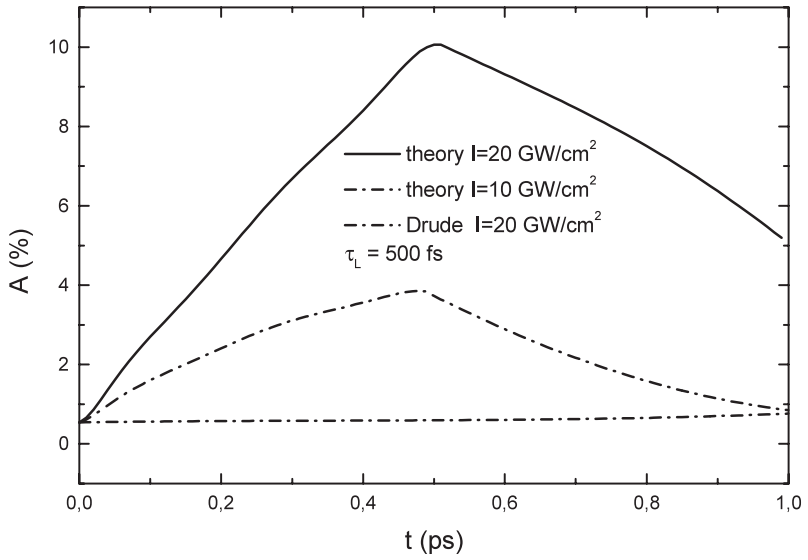

Figure 10. The absorption: full and dashed curves display the theory up to second order; the dash–dotted curve shows Drude's theory.

Next, we give a direct comparison of the theory with experiments. From figures 5 and 6 or from table 1, it follows that the relative change of the imaginary part of the dielectric function is much larger than that of the real part. This outcome agrees well with the experimental findings reported by Elsayed-Ali *et al* (1991). The authors found for gold films that in response to a fs laser pulse the imaginary part of the dielectric function undergoes a significantly higher perturbation than the real part. Moreover, using the experimental data for the fluence, $F = 4$ mJ cm^{-2}, the pulse duration, $\tau_L = 150$ fs, and the photon frequency, $\omega = 2$ eV, which is well below the interband transition energy, we find for the maximal deviations $\Delta\varepsilon_1/\varepsilon_1 = -7.4 \times 10^{-3}$ and $\Delta\varepsilon_2/\varepsilon_2 = 0.56$, which exactly correspond to the difference of two orders seen in the experiment.

Hohlfeld *et al* (1996) carried out a measurement of the relative change of the transient thermal reflectivity of gold for a p-polarized wave with $I = 10$ GW cm^{-2}, $\tau_L = 100$ fs, and $\omega = 2$ eV at incident angles of 43° (pump) and 48° (probe). The results, together with our theoretical calculations, are plotted in figure 11. From the inset we recognize that the alteration of the absorption at early times is primarily governed by the electron temperature; at later times, however, the contribution from the electron–phonon scattering becomes more pronounced due to the rise of the phonon temperature and the fall of the electron one.

3. Conclusion

The nonequilibrium distribution of the electrons and the existence of different temperatures for the electron and phonon subsystems are surely the most essential features appearing in the interaction of fs laser pulses with matter. Although both effects appear also in the case of low intensities (Fann *et al* 1992), their consequences become, of course, more pronounced at high intensities. The replacement of the Fermi–Dirac function by the nonequilibrium distribution function expands the available phase space for the electrons and brings additional terms into the equations. On the other hand, the decoupling of the temperatures enhances the effect of electron–electron scattering. At high electron temperatures, the electron–electron scattering

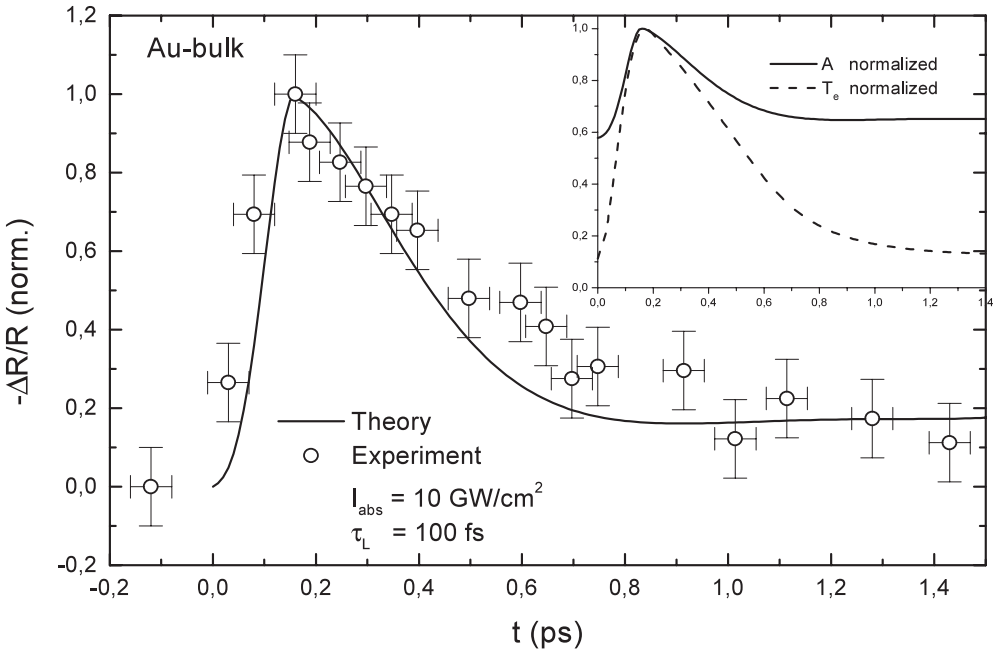

Figure 11. Relative changes of the transient thermal reflectivity of gold for p-polarized light with $\omega = 2$ eV at incident angles of 43° (pump) and 48° (probe). Inset: the normalized absorption and normalized electron temperature.

rate becomes comparable to or even greater than the electron–phonon scattering rate and starts dominating the interactions. Together with the larger phase space, this outcome is responsible for the qualitative and quantitative changes of the optical properties discussed in this paper and for the thermal conductivity investigated by Hüttner (1998). It is worth noting that the new properties are mainly common to all metals and not restricted to the noble metals often considered in pump-and-probe experiments.

A complete self-consistent modelling of the electron and phonon temperatures including the full temperature dependence of all material properties involved represents a formidable mathematical challenge and is still a completely open issue.

References

Banyai N C, Anacker D C, Wang X Y, Reitze D H, Focht G B, Downer M C and Erskine J 1990 *Proc. 7th Int. Conf. on Ultrafast Phenomena* p 116

Bonn M, Denzler D N, Funk S, Wolf M, Wellershoff S S and Hohlfeld J 2000 *Phys. Rev.* B **61** 1101

Elsayed-Ali H E, Juhasz T, Smith G O and Bron W E 1991 *Phys. Rev.* B **43** 4488

Fann W S, Storz R, Tom H W K and Bokor J 1992 *Phys. Rev.* B **46** 13 592

Fedosejevs R, Ottmann R, Sigel R, Kühnle G, Szatmari S and Schafer F P 1990 *Appl. Phys.* B **50** 79

Hohlfeld J, Conrad U and Matthias E 1996 *Appl. Phys.* B **63** 541

Hüttner B 1998 *J. Phys.: Condens. Matter* **10** 6121

Hüttner B 1999 *J. Phys.: Condens. Matter* **11** 6757

Hüttner B and Rohr G 1996 *Appl. Surf. Sci.* **103** 269

Parkins G R, Lawrence W E and Christy R W 1981 *Phys. Rev.* B **23** 6408

Sun C K, Vallee F, Acioli L H, Ippen E P and Fujimoto J G 1994 *Phys. Rev.* B **50** 15 337